Quantitative Analysis of Rectus Extraocular Muscle Layers in Monkey and Humans

Sei Yeul Oh,[1,3] *Vadims Poukens,*[1] *and Joseph L. Demer*[1,2]

Purpose. Rectus extraocular muscles (EOMs) consist of orbital (OL) and global (GL) layers. This study enumerated the fibers in both layers along the length of each EOM.

Methods. Four human (ages 17 months–93 years) and three monkey (ages 5–7 years) orbits were serially sectioned in the coronal plane and stained with Masson's trichrome. All fibers of the rectus EOMs were counted using light microscopy at midorbit in all specimens and regular intervals throughout the orbits for one human and one monkey.

Results. In the GL, human EOMs in midorbit contained 8000 to 16,400 fibers, and monkey EOMs contained 3600 to 6600 fibers, varying little among the four rectus EOMs. In humans and monkeys, the number of OL fibers in midorbit varied widely according to specific EOM, being most numerous for the medial rectus (human: 7400–14,600; monkey: 3700–7000). The GL existed over the entire extent of each EOM from origin in the orbital apex into continuity with the tendon inserting on the globe. The OL was absent in the most anterior portion of each EOM, because OL fibers inserted on the respective EOM pulley.

Conclusions. Primate EOMs contain substantial numbers of OL fibers. Numerical similarity of GL fibers is consistent with similar mechanical loading on each of the four rectus EOMs, as required to rotate the globe. Numerical dissimilarity of OL fibers correlates with varying mechanical loading because of varying elasticities of connective tissues onto which these fibers insert. (*Invest Ophthalmol Vis Sci.* 2001;42:10–16)

Mammalian extraocular muscles (EOMs) have been the subjects of morphologic,[1–3] electrophysiological,[4] and pharmacological studies.[3] Light and electron microscopic studies demonstrate complex fiber composition of EOMs, highly specialized striated muscles having a higher innervation ratio and more variation in fiber size and types than skeletal muscles.[1–3] The EOMs are among the fastest muscles in mammals. Yet, in addition to twitch muscle fibers that are typical of mammalian skeletal muscle, EOMs possess slow fibers that are more characteristic of avian and amphibian muscles.[2,3] It is perhaps because of this paradoxical complexity in their structure that a fundamental enigma remains: specific functions for the wide variety of EOM fibers are unknown.

From the Departments of [1]Ophthalmology and [2]Neurology, the Jules Stein Eye Institute, University of California, Los Angeles; and [3]Department of Ophthalmology, Samsung Medical Center, Sungkyunkwan University School of Medicine, Seoul, Korea.

Supported by National Eye Institute Grant EY-08313 and Core Grant EY-00331. JLD received a Research to Prevent Blindness Lew R. Wasserman merit award and is Laraine and David Gerber Professor of Ophthalmology.

Submitted for publication January 26, 2000; revised May 18, and August 16, 2000; accepted October 10, 2000.

Commercial relationships policy: N.

Corresponding author: Joseph L. Demer, Jules Stein Eye Institute, 100 Stein Plaza, UCLA, Los Angeles, CA 90095-7002. jld@ucla.edu

The EOMs can be divided into two distinct layers.[1–3] The peripheral orbital layer (OL) lies along the EOM surface facing the orbital wall. This layer encloses a second portion, the global layer (GL), closer to globe. The OL contains small-diameter fibers with many mitochondria and abundant vessels. The GL contains larger-diameter fibers with variable mitochondrial content and fewer vessels. By Masson's trichrome stain, OL fibers are stained dark red, but GL fibers are stained bright red.

The literature is sparse but controversial regarding whether each EOM fiber runs the entire length of the EOM. If this were true, one would expect to find the same number of fibers in sections taken from the anterior, middle, or posterior portion of each EOM. In cat, fiber counts from middle portion of the inferior oblique muscle have been consistently higher than counts taken from anterior or posterior portions.[5] In rabbit EOMs, the number of fibers decreases gradually at the insertional tendon is approached.[6] This variation suggests that many fibers must originate and terminate at distances less than that from the origin to the insertion of the EOM. However, in another study in cat, all OL fibers reportedly ran from origin to insertion, whereas in the GL only multiply innervated fibers ran the entire length of the EOM.[7] No comparable data are available on primates.

The classical studies of Koornneef indicated stereotypic organization of connective tissues around the EOMs.[8,9] Recent anatomic studies have clarified that each rectus EOM passes through a pulley consisting of an encircling ring or sleeve of collagen, located near the globe equator in Tenon's fascia.[10–13] Pulleys are coupled to the orbital wall, adjacent EOMs, and equatorial Tenon's fascia by bands containing collagen, elastin, and smooth muscle. Abundant elastic fibers in and around pulleys provide reversible extensibility to these resilient tissues.[10–13] Pulleys have important implications for EOM action because the functional origin of an EOM is at its pulley.[10–13] Several lines of evidence, including magnetic resonance imaging (MRI), gross examinations, surgical exposures, and histologic studies in humans and monkeys indicate that the OL of each rectus EOM inserts on its corresponding pulley, rather than on the globe. Only the GL of the EOM inserts via its tendon on the sclera.[13] The "active pulley hypothesis" proposes that, via dual insertions, the GL of each rectus EOM rotates the globe, whereas the OL inserts on its pulley to linearly position it and thus influence EOM rotational axis.[13] This hypothesis suggests that control of EOM pulling direction by the OL is under fine and instantaneous control to vary ocular kinematics for different types of eye movements. It would therefore be expected that the primate OL would contain a substantial number of fibers and that the number of OL fibers in a given rectus EOM might depend on the mechanical properties of that EOM's pulley.

To better understand the functional anatomy of rectus EOM laminae, the present study compared the number of muscle fibers in the GL and OL using serially sectioned monkey and human orbits from diverse individuals.

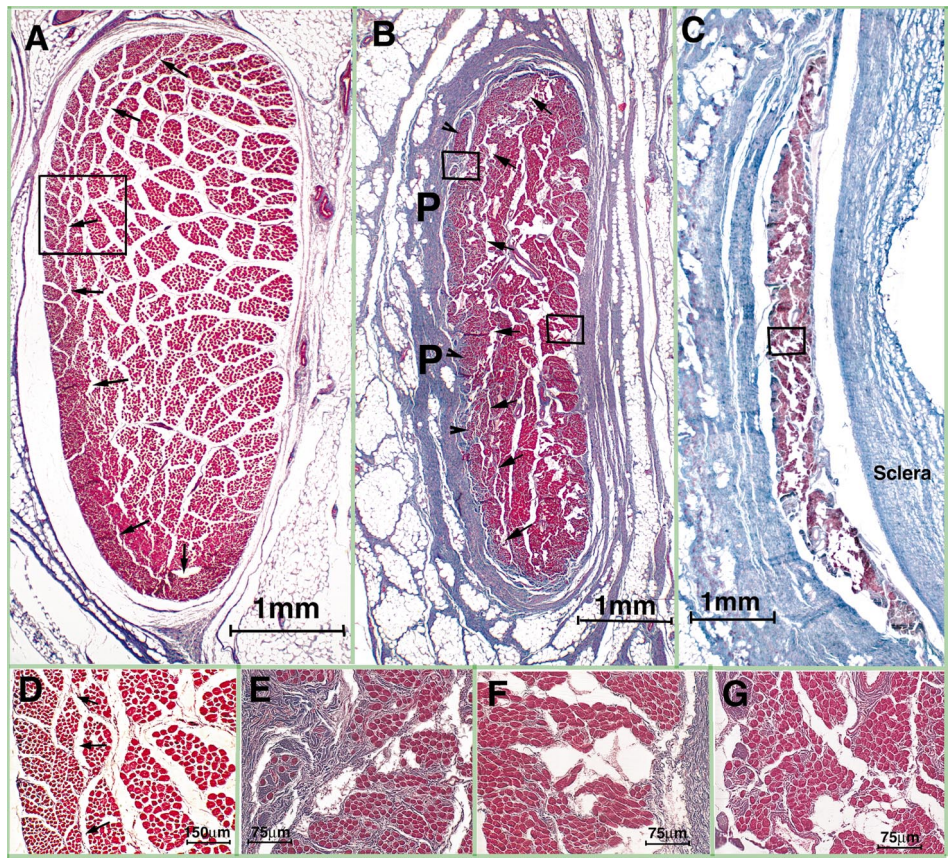

FIGURE 1. Masson's trichrome stain of 10-μm-thick transverse section of medial rectus (MR) muscle. (**A**) Rhesus monkey at low power. The "C" shaped OL is evident on the orbital surface at *left* and stained *dark red*, whereas the GL in the EOM core stains *bright red*. Border is demarcated by *arrows*. *Outlined* region is shown in (**D**). (**B**) Human (age 17 months) at low power at the level of the pulley ring. Fibers in OL (*arrowheads*) insert on the MR pulley (P). The C-shaped OL on the *left* is readily distinguished from the GL. *Right outlined* region at *top left* is shown in (**E**); *bottom right* is shown in (**F**). (**C**) Human (age 17 months) at low power anterior to the pulley. Only the GL is present at this level, as can be verified at higher power in the magnified *inset* shown in (**G**). (**D**) Rhesus monkey at high power. Fibers are smaller in the OL than the GL. Border is demarcated by *arrows.* (**E**) Human OL at high power. Fibers are small and stained *dark red.* OL fibers insert anteriorly into dense collagen (*blue*) of the MR pulley. (**F**) Human GL at high power within the pulley ring. Fibers are large, stain *bright red*, and do not insert on the pulley ring. (**G**) Human GL at high power, anterior to the pulley ring. The larger *red fibers* are typical of the GL.

METHODS

Specimens representing a broad variety of species and ages were obtained to determine fundamental EOM anatomy. Three young adult monkeys (5–7 years old), two rhesus (*Macacca mulatta*) and one fascicularis (*Macacca fascicularis*), and four humans (17 months–93 years old) were studied. All monkeys were handled under a protocol approved by institutional animal welfare committees and adhering to the ARVO Statement for the Use of Animals in Ophthalmic and Vision Research. All human specimens were obtained from cadavers in conformity with legal requirements. Monkeys were euthanatized by IV barbiturate overdose and immediately perfused with warm saline followed by neutral buffered paraformaldehyde (4%). The heads were postfixed for several days in 10% neutral buffered formalin, and the right orbital contents were removed in continuity with the lids and adjacent orbital bones. The head of a 17-month-old male human was freshly frozen to −78°C within 24 hours of death by accidental asphyxiation and was obtained by anatomic donation to a tissue bank (IIAM, Scranton, PA). The head was slowly thawed in 10% neutral buffered formalin for 1 week. Other human orbits were obtained during authorized autopsy from three human cadavers within 12 hours of death. The remaining preparation was similar for monkey and human specimens. Under magnification, the orbits were removed in continuity with the lids and orbital bones, which were thinned from the external surface using a high-speed drill to preserve osseous integrity and mechanical support. The orbits were then lightly decalcified for 24 hours in 0.003 M EDTA and 1.35 N HCL, embedded in paraffin in a vacuum chamber, serially sectioned in the coronal plane at 10-μm thickness, and mounted on 50 × 75 mm gelatin-coated glass slides before staining with Masson's trichrome to define muscle fibers and collagen. All fibers of four rectus EOMs were counted using light microscopy and a hand-held digital counter at midorbit in all specimens. In addition, all fibers were counted throughout the full posterior to anterior extent of each EOM at 2-mm intervals in one rhesus monkey and 3-mm intervals in the 17-month-old human. No sampling or approximations were used. For an estimate of accuracy, duplicate counts were done for three EOMs in three sections more than 2 weeks after the initial counting. Counts were repeatable to within less than 5% (range, 1.1%–4.7%). Comparisons were considered statistically significant for parametric tests when $P < 0.05$, but exact probabilities were computed for rank order comparisons where the number of observations was equal to the number of specimens.

Estimates of fiber diameters were obtained from 24-bit color digital micrographs taken with an Olympus BH-2 microscope fitted with a digital camera (Leaf Lumina; ScyTech, Bedford, MA) having resolution of 3400 × 2800 pixels. Only transversely sectioned fibers were measured, but most fibers nevertheless had roughly elliptical cross sections. Measurements of the greatest diameter of each of 100 randomly selected fibers from each lamina of interest were made using the program NIH Image (W. Rasband, National Institutes of Health; available by ftp from zippy.nimh.nih.gov or floppy disc from NTIS, 5285 Port Royal Road, Springfield, VA 22161; part number PB95-500195GEI).

RESULTS

The C-shaped OL on the orbital surface of each rectus EOM (Figs. 1A, 1B) was readily distinguished from the central GL on the basis of smaller fiber size and darker red staining in the former and the larger, bright red fibers in the latter (Figs. 1D through 1G). The microscopic appearance of the human rectus EOMs was similar to that of the monkey. The OL originated in the orbital apex and coursed anteriorly through the orbit until reaching the sleeve-like pulley of each EOM, an anteroposteriorly distributed structure on which the OL fibers inserted (Figs. 1B, 1E). Global layer fibers did not insert on the pulleys (Fig. 1F), whereas OL fibers were not continuous with the EOM

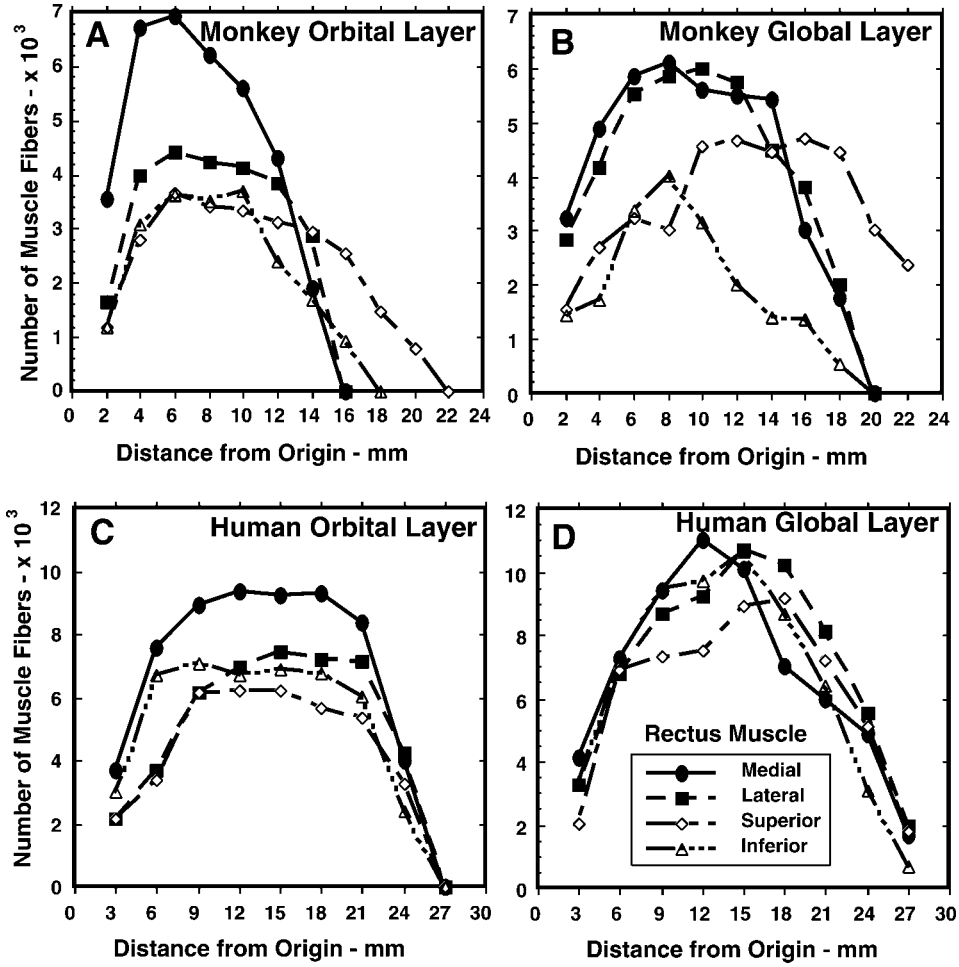

FIGURE 2. Number of fibers the layers of the rectus EOMs of the monkey and human at intervals through the orbit. The MR had the most fibers among the rectus EOMs. (**A**) OL of rhesus monkey. The number of fibers was constant in midorbit for each EOM but varied widely according to individual EOM. (**B**) GL of rhesus monkey. The two horizontal rectus EOMs had similar maximum numbers of fibers, whereas the two vertical rectus EOMs had similar maximum numbers of fibers. For each EOM, the number of fibers varied along its length. Note that for each EOM, fibers were present at distances from the origin where OL fibers had declined to zero. (**C**) OL of 17-month-old human. The number of fibers was constant in midorbit for each EOM, but varied widely according to individual EOM. (**D**) GL of 17-month-old human. All four rectus EOMs had similar maximum numbers of fibers. For each EOM, the number of fibers varied along its length. Note that for each EOM, fibers were present at distances from the origin where OL fibers had declined to zero.

tendons that inserted onto the sclera. The GL extended over the entire length of each rectus EOM, continued through the pulley without inserting (Fig. 1F), and was contiguous with its tendonous insertion on the sclera (Figs. 1C, 1G). The separate insertions of the OL and GL have been demonstrated elsewhere for humans using longitudinal sectioning and elastin staining.[13]

Monkey Specimens

Counting of fibers throughout the orbit in one monkey specimen indicated that the maximum number in both layers occurred roughly in midorbit (Figs. 2 A, 2B). On this basis, fiber numbers were determined for the remaining two monkey specimens in the midorbit. For purposes of counting, the midorbit was taken to be the midpoint between the anterior termination of the myofibers on the tendon, and their posterior origin in the orbital apex. The rectus EOM fibers in the midorbit of the two layers are enumerated in Table 1. Analysis of variance including layers showed a significant variation according to specific rectus EOM ($P < 0.05$). Among the four rectus EOMs, the variation in the number of fibers according to specific EOM in the GL was smaller than for the OL. This behavior was quantified by computation for each of the four

TABLE 1. Number of Monkey Rectus Muscle Fibers

Animal	Medial Rectus	Lateral Rectus	Superior Rectus	Inferior Rectus	Coefficient of Variation
A. *Global Layer*					
Rhesus 1	6121	5983	4698	4040	0.19
Rhesus 2	6653	6060	4805	5705	0.13
Fascicularis	4929	4762	3655	4303	0.13
Mean ± SD	5901 ± 883	5602 ± 728	4386 ± 635	4683 ± 895	0.15 ± 0.04
B. *Orbital Layer*					
Rhesus 1	6935	4403	3670	3697	0.33
Rhesus 2	7013	5139	4873	5185	0.18
Fascicularis	3702	3108	2432	2901	0.17
Mean ± SD	5883 ± 1889	4217 ± 1028	3658 ± 1221	3928 ± 1159	0.23 ± 0.09

TABLE 2. Medial Rectus Muscle Fiber Diameters

	17 Months		4 Years		57 Years		93 Years	
	Global	**Orbital**	**Global**	**Orbital**	**Global**	**Orbital**	**Global**	**Orbital**
Mean	15.00	10.80	17.60	10.50	19.00	12.10	16.20	11.60
SD	4.00	2.70	3.00	1.90	5.90	2.00	5.10	3.40
Median	15.10	10.30	17.40	10.60	18.70	12.00	16.30	11.50
SEM	0.40	0.27	0.30	0.18	0.59	0.19	0.51	0.34

The sample consisted of 100 fibers from midorbit. Values are expressed in micrometers.

rectus EOMs the coefficient of variation (CV), which is the SD divided by the mean of the number of fibers. The mean CV among all monkeys was 0.15 in the GL and 0.23 in the OL, and the CV for every individual animal was greater in the OL than in the GL (Table 1). Assuming a binomial distribution for the sample size of three orbits, the odds of this occurring by chance are only one in no more than eight. In the GL, the medial rectus (MR) in every specimen had the most numerous fibers at a mean of 5901 ± 883 (mean ± SD), followed in every specimen by the lateral rectus (LR) at a mean of 5602 ± 728. The two vertical rectus EOMs followed in variable order depending on the specimen, with the superior rectus (SR) having the least average number at 4386 ± 635 (Table 1). χ^2 testing indicated that this distribution is extremely improbable based on chance ($P < 0.001$). In the OL of every specimen, the MR also had the most numerous fibers at a mean of 5883 ± 1889, followed by the LR at a mean of 4217 ± 1028, the inferior rectus (IR) at a mean of 3928 ± 1159, and the SR at a mean of 3658 ± 1221 (Table 1). This distribution is also extremely improbable based on chance ($P < 0.001$).

The horizontal rectus EOMs had closely matched numbers of GL fibers (Fig. 2B, Table 1), with no statistically significant difference between MR and LR ($P > 0.05$, Student-Newman-Keuls test). The vertical rectus EOM had fewer GL fibers than the horizontal rectus EOMs, but the numbers in the pair were also roughly matched to one another (Fig. 2B). There was no statistically significant difference between IR with SR muscles, but there was a statistically significant difference between the horizontal and vertical rectus muscles ($P < 0.05$, Student-Newman-Keuls test). The number of rectus EOMs fibers appeared to differ in the two monkey species. The two rhesus monkeys had similar numbers of fibers in the two layers but had more numerous muscle fibers than the fasciculalis monkey (Table 1). Sample size is insufficient to test for statistical significance of a possible species difference.

Human Specimens

The qualitative impression of larger fibers in the GL was validated by measurement of greatest diameters of 100 fibers randomly sampled from a section from the midorbital region of the MR of each human specimen. Fiber diameters are shown in Table 2. Although there was modest variation in mean fiber diameter among specimens, GL fiber diameter was in every case significantly greater than OL fiber diameter within specimens ($P < 0.05$; Student's *t*-test).

In the 17-month-old human, fibers in the both layers were enumerated at 3-mm intervals along the length of each EOM. Counting of fibers throughout the orbit in this specimen indicated that, as in monkey, the maximum number in both layers occurred roughly in midorbit (Figs. 2C, 2D). In the human, the number of OL fibers was roughly constant in the middle of the anteroposterior length of each EOM, as indicated by the flat central zone in Figure 2C. There was a decline in fiber numbers at the anterior and posterior ends of each EOM. As in monkey, the OL did not continue to the anterior to the pulley of any rectus EOM, because it inserted on the corresponding pulley (Fig. 1C).[13] The collagen content of the pulley rings was similar among all human specimens. The number of GL fibers in each EOM reached a maximum in midorbit, with a graded decline both anteriorly and posteriorly (Fig. 2D). The GL was present over the entire length of each rectus EOM, continuing anterior to the termination of the OL (Fig. 2C), and contiguous with its tendonous insertion on the sclera as described elsewhere.[13] The more anterior extent of the GL may be appreciated quantitatively by noting that, for each of the four rectus EOMs, the number of GL fibers (Fig. 2D) exceeds zero at the anterior location where the number of OL fibers (Fig. 2C) has declined to zero.

Based on the preceding data, the midorbital region was chosen to determine fiber numbers for the remaining three

TABLE 3. Number of Human Rectus Muscle Fibers

Age	Medial Rectus	Lateral Rectus	Superior Rectus	Inferior Rectus	Coefficient of Variation
A. *Global Layer*					
17 Months	11,044	10,692	9,198	10,620	0.08
4 Years	16,404	15,674	12,270	14,680	0.12
57 Years	15,294	14,416	12,311	14,120	0.09
93 Years	9,492	9,693	8,035	8,755	0.08
Mean ± SD	13,059 ± 3,315	12,619 ± 2,877	10,454 ± 2,174	12,044 ± 2,835	0.09 ± 0.02
B. *Orbital Layer*					
17 Months	9,377	7,456	6,237	7,074	0.18
4 Years	14,203	11,834	9,289	11,163	0.17
57 Years	14,658	11,090	8,697	10,450	0.22
93 Years	7,432	5,789	4,749	6,023	0.18
Mean ± SD	11,418 ± 3,573	9,042 ± 2,892	7,243 ± 2,124	8,678 ± 2,512	0.19 ± 0.02

human specimens. For purposes of counting, the midorbit was taken to be the midpoint between the anterior termination of the myofibers on the tendon and their posterior origin in the orbital apex. In both layers of every specimen, the MR had the most fibers, followed by the LR, IR, and SR, in that order. χ^2 testing indicates that this sequence is extremely improbable on the basis of chance ($P < 0.001$). Among specimens, the number of midorbital rectus EOM fibers ranged from 8035 to 16,404 in the GL (Table 3) and from 4749 to 14,658 in the OL (Table 3). As in monkey, the variation in fiber number among the four rectus EOMs was greater in the OL than in the GL (Table 3). The mean CV was 0.09 in the human GL and 0.19 in the OL, and in every specimen the CV for the GL was less than for the OL (Table 3). Based on a binomial distribution, the odds of this occurring by chance in the humans are no more than 1 in 16, the most stringent level of significance possible with four specimens. If human and monkey specimens are pooled for this statistical consideration, the difference in CV between the GL and OL is significant at the 0.008 level. However, unlike monkeys in which the number of GL fibers in the horizontal and vertical rectus pairs was matched, in humans the number of midorbital fibers in the GL of all four rectus EOMs was roughly similar at a mean of 12,044 ($P > 0.05$, Student-Newman-Keuls test). The number of fibers in the OL varied more substantially, with a maximum 11,418 ± 3573 (mean ± SD) for the MR, followed by 9042 ± 2892 for the LR, 8678 ± 2512 for the IR, and 7243 ± 2124 for the SR (Table 3). However, this variation in number of OL fibers was not statistically significant by analysis of variance ($P > 0.05$).

The orbits from 4- and 57-year-old specimens had numbers of fibers similar to each other in both the GL and OL, but fibers were more numerous than from specimens 17 months or 93 years old (Table 3). The number of specimens is insufficient to determine whether this apparent variation with age is systematic.

Discussion

In the midorbital portions of the rectus EOMs, the OL contained 39% to 53% of the total number of muscle fibers in the monkey specimen (Table 1) and 37% to 49% in the human (Table 3). This extends to primates the findings reported in rat,[14] rabbit,[15] and cat[5] that the OL contained 30% to 49% of total number of EOM fibers. The abundance of its fibers across species and subject ages is consistent with an important role for the OL in ocular motility.

Orbital layer fibers were entirely absent in the terminal anterior portions of the EOMs in both monkey and human, confirming the results of longitudinal sectioning indicating that OL fibers do not insert on sclera.[13] This is also consistent with the finding in rabbit that the inner OL does not reach the tendon end.[6] Rectus EOMs are encircled by fibromuscular pulleys consisting of a ring within a sleeve of collagen (Fig. 1B) located near equator of the globe in Tenon's fascia.[10,12,13] Pulley sleeves have a broad anteroposterior extent exceeding 10 mm, partially accounting for the gradual anterior decline to zero in the number of OL fibers (Figs. 2A, 2C). Pulleys are coupled to the orbital wall, adjacent EOMs, and equatorial Tenon's fascia by bands containing collagen, elastin, and smooth muscle. The amount of fibromuscular connective tissue in its suspension depends on the particular rectus pulley, with the MR pulley contains the greatest amount of fibroelastic tissue and smooth muscle and the SR the least. The existence of a pulley dissociates the anatomic origin of an EOM in the orbital apex from its functional mechanical origin at the pulley, which determines the EOM's pulling direction. The present study confirms that OL fibers of each rectus EOM insert, not on the sclera, but on the corresponding pulley.[13] MRI of human rectus EOM path inflections and the insertion of OLs on the pulleys indicates that the pulleys make large anteroposterior translations along the EOM axes during gaze shifts.[13] Each pulley shifts posteriorly with contraction of its OL and shifts anteriorly as relaxation of its OL allows the elastic pulley suspension passively to move the pulley toward the orbital rim. According to the active pulley hypothesis, this anteroposterior translation of the pulley is mechanically required to properly control the rotational axis of the EOM to implement behavior of the peripheral ocular motor apparatus that has favorable kinematic properties. These favorable properties include conformity to Listing's law, which states that, with the head upright and stationary, all rotational axes of the eye lie in a plane.[13] In general, the orientation of a solid object depends on the order of rotations; however, appropriate positioning of pulleys makes eye orientation relative to neural commands effectively independent of the order of rotations and thus "rotationally commutative."[16] Because pulley locations are under active control by the balance of OL muscle tone against the elasticity of the pulley suspensions, these locations cannot be accurately determined in cadaveric material, particularly if the EOMs have been dissected free of pulley suspensions. Mean human rectus pulley locations have been determined in vivo by MRI imaging of EOM path inflections in secondary gaze positions, and the locations are consistent with the average location of Listing's plane.[17]

Among the four rectus EOMs the number of OL fibers was greatest in the MR muscle in both the monkey and human orbits. In the monkey OL, the mean number of MR fibers (5883) was 61% more than the mean number of orbital SR fibers (3658). In the human OL, the mean number of MR fibers (11,418) was 58% more than the mean number of orbital SR fibers (7243). This variation is consistent with the distribution of connective tissue in the pulley suspensions of the four rectus EOMs,[10] constituting the elastic load on the pulleys.[13] The systematic variation in the number of fibers in the OL contrasts with the consistent numbers in the GL, where in the human the mean number of fibers was equal within about ±15% among the four rectus EOMs. This finding suggests that the mechanical load on GL fibers is similar for all EOMs, as might be expected because these fibers insert on the globe.

Electromyographic (EMG) recordings in the GL of the human LR demonstrated both a phasic pulse and tonic step of activity during saccades, the former being necessary to drive the formidable viscous load imposed by the relaxing antagonist EOM and the latter necessary to oppose the lesser elastic load as fixation is maintained.[18] Recordings of tension in the insertional tendons of horizontal rectus EOMs of behaving monkeys confirm the presence of both saccadic pulses and steps.[19] In the OL, however, EMGs showed essentially only a step of activity during saccades.[18] Fibers in the OL have lower recruitment thresholds than those in the GL, with most OL fibers active throughout the oculomotor range and most GL fibers active only in their fields of action.[18] This latter observation motivated Collins[18] to suggest long ago that the OL might have a special role in fixation, with the GL participating preferentially in dynamic eye movements. The contemporary insight that the OL inserts on the pulley rather than on the globe permits a more satisfactory understanding of these observations. The mechanical load on the OL is dominated by elasticity of the pulley suspension. Collins[18] has pointed out that the main load on EOMs attached to the globe is viscosity arising from the relaxing antagonist. A pulse of force is unnecessary in the OL to achieve brisk pulley motion against a mainly elastic load. This elastic loading of the pulley by connective tissue requires that OL fibers maintain active tension throughout the oculomotor range to avoid any region of slack. In contrast, GL

fibers remain under tension even when relaxed because they are passively stretched by the antagonist EOM. These considerations explain the EMG observations of Collins that fibers in the OL are active throughout the entire oculomotor range, whereas most GL fibers become silent only slightly out of their field of action.[18] With these concepts in mind, it is easy to understand the extensive development of the OL in primates.

Approximately 80% of fibers in the OL of each EOM are fast, twitch-generating, singly innervated fibers (SIFs) resembling mammalian skeletal muscle fibers, whereas 20% are multiply innervated fibers (MIFs) that either do not conduct action potentials or do so only in their central portions.[3] Orbital SIFs are specialized for intense oxidative metabolism and fatigue resistance[3] and presumably provide most of the force required of the OL to maintain tension against the elastic pulley suspensions. In cat the most powerful and fatigue resistant motor units of the LR muscle, comprising of 27% of all units, consist of single neurons innervating fibers in both the OLs and GLs.[20] Such "bilayer units" are likely to participate in the coordination of anteroposterior pulley position, with ocular rotation required for consistency with the kinematic requirements of Listing's law of ocular torsion.[13] The function of the relatively sparse and primitive orbital MIFs remains unclear.

Approximately 90% of fibers in the GL are fast, twitch-generating SIFs, whereas 10% are slow, nontwitch MIFs resembling those of amphibians.[3] The SIFs are often divided into three types, red, intermediate, and white, distinguished by their density of mitochondria and fatigue resistance.[3] The largest and most granular red SIFs, constituting approximately 33% of all global fibers, are very similar to orbital SIFs and are highly fatigue resistant, whereas the intermediate and white SIFs have progressively lower fatigue resistance.[3] The predominant static loading of the GL by the moderate contractile force of antagonist EOM accounts for the GL's higher overall recruitment threshold than the OL[18] and the lesser oxidative, vascular, and fatigue-resistant features of orbital SIFs.[3] However, during saccades the high viscous loading of the GL by the relaxing antagonist EOM requires the high transient force that intermediate and white SIFs are well suited to provide. In the GL of monkey rectus EOMs, 80% of MIFs terminate in innervated myotendinous cylinders at the musculotendinous junction called palisade endings (PEs).[21] Similar PEs have been demonstrated in all human EOMs.[22] Although their potential for proprioception has been controversial,[21,23] studies in cat confirm PEs to be sensory.[24] Human EOMs also contain neuromuscular spindles that are thought to be sources of proprioceptive input to the brain,[25] although the EOMs of monkeys are poorly endowed with spindles.[26] A careful study based on serial sections of isolated human EOMs from orbits more than 65 years of age demonstrated a mean of 16 to 34 spindles per rectus and four per oblique EOM.[25] In humans, spindles occur mainly in the proximal and distal regions at the border between the OL and the GL.[2,23,25]

The literature is contradictory regarding whether OL fibers are continuous from their origin in the orbital apex to their insertion in the anterior site now interpreted to be the pulley. Mayr et al.[7] reported that the feline OL fibers run the entire extent of the EOM, but Alvarado and Van Horn[5] found a variation in fiber number along the length of the inferior oblique muscle of cat. Gradual distal reduction in the number of fibers of IR and LR fibers has been reported for the rabbit.[6] Although the present data in the human (Fig. 2C) suggest a region of relative constancy in the number of fibers in each of the rectus EOMs in the region 9 to 21 mm from the orbital apex, no zone of relative constancy is evident for the monkey MR (Fig. 2A). In both human and monkey specimens there is a gradual decline in the number of fibers over approximately the anterior 6 mm of the OL and the anterior 4 to 12 mm of the GL. The variation in the number of fibers along the length of an EOM suggests that the fibers posteriorly bifurcate and more anteriorly reunite in myomyous junctions.[6] The presence of branching and myomyous junctions has important physiologic implications, because these properties would result in nonlinear force addition as has been observed during stimulation of small numbers of EOM motor units in monkey.[27,28] Because human rectus EOMs have the same numerical evidence of bifurcation and myomyous junctions, the present study extends the likelihood of nonlinear summation of EOM fiber tension to humans as well. Nonlinear summation of motor unit tension should be considered in quantitative modeling of the human ocular motor system.

References

1. Durston JHJ. Histochemistry of primate extraocular muscles and changes of denervation. *Br J Ophthalmol.* 1974;58:193–216.
2. Spencer RF, Porter JD. Structural organization of the extraocular muscles. In: Buttner-Ennever J, ed. *Neuroanatomy of the Oculomotor System*. Amsterdam: Elsevier; 1988:33–79.
3. Porter JD, Baker RS, Ragusa RJ, Brueckner JK. Extraocular muscles: basic and clinical aspects of structure and function. *Surv Ophthalmol.* 1995;39:451–484.
4. Chiarandini DJ, Kaiser KK. Electrophysiological identification of two types of fibres in the rat extraocular muscles. *J Physiol.* 1979;290:453–465.
5. Alvarado J, Van Horn C. Muscle cell types of the cat inferior oblique. In: Lennerstrand G, Bach-y-Rita P, eds. *Basic Mechanisms of Ocular Motility and Their Clinical Implications*. New York: Pergamon Press; 1975:15–43.
6. McLoon LK, Rios L, Wirtschafter JD. Complex three-dimensional patterns of myosin isoform expression: differences between and within specific extraocular muscles. *J Muscle Res Cell Motil.* 1999; 20:771–783.
7. Mayr R, Sottwchall J, Gruber H, Neuhuber W. Internal structure of cat extraocular muscle. *Anat Embyol.* 1975;148:24–34.
8. Koornneef L. The architecture of the musculo-fibrous apparatus in the human orbit. *Acta Morphol Neerl Scand.* 1977; 15:35–64.
9. Koornneef L. Orbital septa: anatomy and function. *Ophthalmology.* 1979;86:876–880.
10. Demer JL, Miller JM, Poukens V, Vinters HV, Glasgow BJ. Evidence for fibromuscular pulleys of the recti extraocular muscles. *Invest Ophthalmol Vis Sci.* 1995;36:1125–1136.
11. Demer JL, Miller JM, Poukens V. Surgical implications of the rectus extraocular muscle pulleys. *J Pediatr Ophthalmol Strabismus.* 1996;33:208–218.
12. Demer JL, Poukens V, Miller JM, Micevych P. Innervation of extraocular pulley smooth muscle in monkeys and humans. *Invest Ophthalmol Vis Sci.* 1997;38:1774–1785.
13. Demer JL, Oh SY, Poukens V. Evidence for active control of rectus extraocular muscle pulleys. *Invest Ophthalmol Vis Sci.* 2000;41: 1280–1290.
14. Vita GF, Mastaglia FL, Johnson MA. A histochemical study of fibre types in rat extraocular muscles. *Neuropathol Appl Neurobiol.* 1980;6:449–463.
15. Barmack NH. Laminar organization of the extraocular muscles of the rabbit. *Exp Neurobiol.* 1978;59:304–321.
16. Quaia C, Optican LM. Commutative saccadic generator is sufficient to control a 3-D ocular plant with pulleys. *J Neurophysiol.* 1998; 79:3197–3215.
17. Clark RA, Miller JM, Demer JL. Three-dimensional location of human rectus pulleys by path inflections in secondary gaze positions. *Invest Ophthalmol Vis Sci.* 2000;41:3787–3797.

18. Collins CC. The human oculomotor control system. In: Lennerstrand G, Bach-y-Rita P, eds. *Basic Mechanisms of Ocular Motility and Their Clinical Implications*. New York: Pergamon; 1975:145–180.
19. Miller JM, Robins D. Extraocular muscle forces in alert monkey. *Vis Res.* 1992;32:1099–1113.
20. Shall MS, Goldberg SJ. Lateral rectus EMG and contractile responses elicited by cat abducens motoneurons. *Muscle Nerve.* 1995;18:948–955.
21. Ruskell GL. The fine structure of innervated myotendinous cylinders in extraocular muscles of rhesus monkeys. *J Neurocytol.* 1978;7:693–708.
22. Richmond FJ, Johnston WS, Baker RS, Steinbach MJ. Palisade endings in human extraocular muscles. *Invest Ophthalmol Vis Sci.* 1984;25:671–676.
23. Ruskell GL. Extraocular muscle proprioceptors and proprioception. *Prog Retinal Eye Res.* 1999;18:269–291.
24. Billig I, Buisseret Delmas C, Buisseret P. Identification of nerve endings in cat extraocular muscles. *Anat Rec.* 1997;248:566–575.
25. Lukas JR, Aigner M, Blumer R, Heinzl H, Mayr R. Number and distribution of neuromuscular spindles in human extraocular muscles. *Invest Ophthalmol Vis Sci.* 1994;35:4317–4327.
26. Maier A, De Ssantis M, Eldred E. The occurence of muscle spindles in extraocular muscles of various vertebrates. *J Morphol.* 1974; 143:397–408.
27. Goldberg SJ, Wilson KE, Shall MS. Summation of extraocular motor unit tensions in the lateral rectus muscle of the cat. *Muscle Nerve.* 1997;20:1229–1235.
28. Goldberg SJ, Meredith MA, Shall MS. Extraocular motor unit and whole-muscle responses in the lateral rectus muscle of the squirrel monkey. *J Neurosci.* 1998;18:10629–10639.